Biochimica et Biophysica Acta 1802 (2010) 331–338

Contents lists available at ScienceDirect

Biochimica et Biophysica Acta

journal homepage: www.elsevier.com/locate/bbadis

Enhanced ROS production by NADPH oxidase is correlated to changes in antioxidant enzyme activity in human heart failure

Elisabetta Borchi [a], Valentina Bargelli [a], Francesca Stillitano [b], Carla Giordano [c], Mariangela Sebastiani [c], Paolo Antonio Nassi [a], Giulia d'Amati [c], Elisabetta Cerbai [b], Chiara Nediani [a,*]

[a] Department of Biochemical Sciences, University of Florence, Viale Morgagni, 50, 50134 Florence, Italy
[b] Department of Preclinical and Clinical Pharmacology, University of Florence, Florence, Italy
[c] Department of Experimental Medicine, La Sapienza University of Rome, Italy

ARTICLE INFO

Article history:
Received 8 September 2009
Received in revised form 13 October 2009
Accepted 28 October 2009
Available online 3 November 2009

Keywords:
NADPH oxidase
Catalase
Glutathione peroxidase
Mn superoxide dismutase
Heart failure

ABSTRACT

In pathological conditions, the balance between reactive oxygen species (ROS) and antioxidants may shift toward a relative increase of ROS, resulting in oxidative stress. Conflicting data are available on antioxidant defenses in human failing heart and they are limited to the left ventricle. Thus, we aimed to investigate and compare the source of oxidant and antioxidant enzyme activities in the right (RV) and left (LV) ventricles of human failing hearts. We found a significant increase in superoxide production only by NADPH oxidase in both failing ventricles, more marked in RV. Despite unchanged mRNA or protein expression, catalase (CAT) and glutathione peroxidase (GPx) activities were increased, and their increases reflected the levels of Tyr phosphorylation of the respective enzyme. Manganese superoxide dismutase (Mn-SOD) activity appeared unchanged. The increase in NADPH oxidase-dependent superoxide production positively correlated with the activation of both CAT and GPx. However, the slope of the linear correlation (m) was steeper in LV than in RV for GPx (LV: $m=2.416$; RV: $m=1.485$) and CAT (LV: $m=1.007$; RV: $m=0.354$). Accordingly, malondialdehyde levels, an indirect index of oxidative stress, were significantly higher in the RV than LV. We conclude that in human failing RV and LV, oxidative stress is associated with activation of antioxidant enzyme activity. This activation is likely due to post-translational modifications and more evident in LV. Overall, these findings suggest a reduced protection of RV against oxidative stress and its potential contribution to the progression toward overt heart failure.

1. Introduction

Myocardial oxidative stress due to increased generation of reactive oxygen species (ROS) plays a recognized role in the pathogenesis as well as the progression of heart failure (HF) [1–4]. The myocardium is equipped with a variety of endogenous enzymatic and non-enzymatic antioxidant systems that are sufficient to metabolize ROS. In particular, superoxide dismutase (SOD), glutathione peroxidase (GPx) and catalase (CAT) counteract the cytotoxic effects of reactive oxygen metabolites [5]. In HF, an imbalance between ROS production and cellular antioxidant defenses might influence myocardial function deterioration and disease progression [6]. Potential sources of increased ROS generation in failing heart include the mitochondria and enzymes, such as xanthine oxidase, cytochrome P450 oxidases, uncoupled NO synthases and NADPH oxidases. Recent studies, including ours, have demonstrated that NADPH oxidase was the major source of ROS in the human failing myocardium and that it was important in the pathogenesis of several aspects of cardiac remodeling largely through actions on redox-sensitive signal transduction [7–10]. To date, a comprehensive view of changes in oxidative stress mechanisms and antioxidant enzyme activity in human HF is far to be completely understood. Moreover, the currently available information is somehow contradictory. For example, CAT activity in the failing human ventricle was reported to be either decreased [11], upregulated [5] or unchanged [12] in different studies. The same studies showed either no change in mRNA, protein levels, SOD and GPx activity [5,6,11] or decreased Mn-SOD activity though in the presence of upregulated mRNA levels [12]. Altogether, they highlight the need to evaluate the oxidative and antioxidant environment in a comprehensive manner and, if possible, to compare alterations occurring in different compartments of the same heart.

In patients with advanced HF, attention has long been attracted by the functional assessment of the left ventricle (LV) with little – if any – interest toward the right one (RV) [13]. Recently, the importance of RV function as a powerful predictor of mortality in HF has been acknowledged [14,15], but little is known about the concomitant cellular and molecular changes occurring in the RV associated with HF. Indeed, only some recent studies inferred that unlike mechanisms account for cardiac hypertrophy and failure in RV and LV [16–18].

* Corresponding author. Tel.: +39 554598321; fax: +39 554598905.
E-mail address: chiara.nediani@unifi.it (C. Nediani).

0925-4439/$ – see front matter © 2009 Elsevier B.V. All rights reserved.
doi:10.1016/j.bbadis.2009.10.014

Differences between the two ventricles were also unraveled by the use of left ventricular assist device (LVAD) as a bridge to heart transplantation or as destination therapy in end-stage HF patients [19]. In fact, despite the general clinical benefit of LVAD [20,21], RV failure after device implantation emerged as a major post-operative problem and is associated with a high mortality rate [22].

In our previous study [10], we demonstrated that oxidative stress resulting from increased ROS generation by NADPH oxidase was present in both ventricles of end-stage human failing heart, but more marked in failing RV. Based on these findings, the present study was aimed at investigating whether the increase in ROS generation in the failing human ventricles was accompanied by changes in antioxidant enzyme expression and/or activity with respect to non-failing (NF) hearts, and to assess whether these changes were equally coordinated in the LV and RV.

2. Materials and methods

2.1. Source of tissue

All patients gave their informed consent prior to their inclusion in the study that conformed to the Declaration of Helsinki and institutional ethical regulations. Explanted failing hearts were obtained from patients undergoing transplantation for end-stage heart failure secondary to idiopathic dilated cardiomyopathy ($n=4$ male, $n=1$ female; mean age 39 years, range 30–60) or ischemic heart disease ($n=6$ male, $n=1$ female; mean age 60 years, range 53–69). All patients were in New York Heart Association class III/IV, with a mean LV ejection fraction of 22% and a mean pulmonary artery pressure of 33 mm Hg. Non-failing (NF) donor hearts ($n=4$ male, $n=3$ female; no cardiac medication; mean age 45 years, range 40–50;) which were unsuitable for transplantation for technical reasons, were used as controls. Clinical characteristics of the three groups are shown in Table 1.

Immediately after explant, myocardial tissue samples were snap-frozen in liquid nitrogen-chilled isopentane for protein, RNA analysis and biochemistry. All tissues were stored at −80 °C. Prior to each experiment, sections stained with hematoxylin–eosin and Masson Trichrome stain was obtained from each sample for morphological examination. Histologic slides from both failing and non-failing hearts were observed under light microscopy.

Table 1
Clinical characteristics of the patients.

	NF	IHD	DCM
Total number	7	7	5
Sex (M/F)	4/3	6/1	4/1
Age (range)	45 (40–50)	39 (30–60)	60 (53–69)
LVEF (%)		23 ± 4.8	20 ± 2.5
CI (l/min/m^2)		2,4 ± 0.2	1.8 ± 0.05
PAP (mm Hg)		38 ± 3.2	29 ± 5.4
PCWP (mm Hg)		24 ± 3	21 ± 5.4
RAP (mm Hg)		15 ± 4.2	10.5 ± 2.3
NYHA class		III–IV	III–IV
Medication			
Diuretics		7	5
Digoxin		0	1
Antiarrhythmics		2	1
ACE-I		7	5
β-blockers		7	5
Nitrates		4	0
HMGCoA-Inh		2	0
ANF/rRNA 18S	1.03 ± 0.001	12.4 ± 1.05	12.3 ± 0.98
MCH-α/rRNA 18S	1.30 ± 0.03	0.06 ± 0.01	0.04 ± 0.002
MCH-β/rRNA 18S	1.35 ± 0.2	0.06 ± 0.02	0.54 ± 0.05

LVEF, left ventricular ejection fraction; CI , cardiac index; ACE-I, angiotensin converting enzyme inhibitors; PAP, pulmonary artery pressure; PCWP, pulmonary capillary wedge pressure; RAP, right atrial pressure; HMGCoA inhibitors (statins); ANF, atrial natriuretic factor; MHC, myosin heavy chain.

Myocyte hypertrophy was a common finding in all failing hearts, associated with variable degrees of interstitial fibrosis, graded from mild (+ 1) to severe (+ 3) on a semi-quantitative basis (not shown). According to the results of the histologic examination, myocardial samples with minimal amounts of fibrosis and devoid of inflammatory infiltrates were selected for molecular and biochemical studies. In addition, expression of atrial natriuretic factor (ANF), and myosin heavy chain (MHC)-α and -β isoforms, molecular markers of cardiac hypertrophy, were evaluated both on NF and failing hearts by RT-PCR using the Platinum SYBR Green qPCR Super Mix- UDG (Invitrogen, Italy) [23].

2.2. Sample preparation

LV and RV samples from NF and failing hearts were homogenized in ice-cold 20 mM Tris–HCl pH 7.4, containing 10 μg/ml leupeptin, 10 μg/ml aprotinin, 0.2 mM PMSF and phosphatase inhibitor cocktail (Sigma, Italy). After spinning for 10 min at 3000 rpm at 4 °C on an Eppendorf Centrifuge 5804 R (Eppendorf, Italy), samples of total heart homogenates were used for NADPH oxidase activity, Western blotting, lipid peroxidation assay and antioxidant enzyme activities. Protein concentration was measured by bicinchoninic acid (BCA) protein assay (Pierce, Italy).

2.3. NADPH oxidase activity

Superoxide production by NADPH oxidase was assessed in tissue homogenates from NF and failing hearts using lucigenin (5 μM)-enhanced chemiluminescence (300 μM NADPH; 100 μg protein / tube), as previously described [10]. Further measurements were taken after the addition of specific inhibitors of oxidase systems: diphenyleneiodonium (DPI, 20 μM), a NADPH oxidase flavoprotein inhibitor, *N*ω-nitro-L-arginine methyl ester hydrochloride (L-NAME, 100 μM), a nitric oxide synthase inhibitor; rotenone (50 μM), a mitochondrial oxidase complex I inhibitor; oxypurinol (100 μM), a xanthine oxidase inhibitor. A cell-permeable superoxide scavenger 4,5-dihydroxy-1,3-benzene-disulfonic acid (Tiron, 20 mM) was also used. A buffer blank was subtracted from each reading. Superoxide production was expressed as an arbitrary light unit over 10 min.

2.4. Nox4 gene expression

Total RNA from each cardiac sample was isolated and DNase-treated with the RNeasy Fibrous Tissue Mini Kit (Qiagen, Italy) following the manufacturer's instructions. Isolated RNA was quantified (spectrophotometric absorbance at 260 nm) and its purity was confirmed by the A260/A280 ratio. The integrity of total RNA was evaluated by ethidium bromide staining on a denaturing agarose gels. RNA samples were stored at −80 °C. Single-stranded cDNA was obtained by using High Capacity cDNA Reverse Transcription Kit (Applied Biosystems, CA, USA) following manufacturer's instructions. Reverse transcription was performed at 25 °C for 10 min and 37 °C for 120 min and stopped by incubating at 85 °C for 5 s. Expression levels of Nox4 gene were investigated using real-time quantitative RT-PCR and TaqMan® probe-based chemistry. Primers and probes for Nox were obtained from ABI (Foster City, CA, USA) TaqMan Gene Expression Assay catalogue. These assays come in a 20× reaction mix, span an exon–exon junction and are optimized to give approximately 100% efficiency. GAPDH was used as a housekeeping gene [Human GAPD (GAPDH) Endogenous Control (VIC / MGB Probe, Primer Limited) Applied BioSystems, CA, USA]. The real-time RT-PCR reactions were carried out using TaqMan® Gene Expression Master Mix (Applied BioSystems, CA, USA) in a 20 μl reaction volume containing 50 ng of cDNA. All reactions were performed in triplicate and included a negative control. PCR reactions were carried out using an ABI Prism 7500 Sequence Detection System (Applied Biosystems, CA, USA).

Cycling conditions were 2 min at 50 °C, 10 min at 95 °C and 40 cycles of 15 s at 95 °C and 1 min at 60 °C. The relative quantification of mRNA levels was obtained by the 7500 system software which uses the comparative method (ΔCT).

2.5. Mn-SOD, GPx and CAT gene expression

Relative expression of Mn-SOD, GPx and CAT genes was determined by quantitative RT-PCR using the Platinum SYBR Green qPCR Super Mix- UDG (Invitrogen, Life Technologies, Paisley, UK). PCR conditions and primers for Mn-SOD and GPx were as previously detailed [23]; for CAT gene expression, we used the following set of primers: forward primer GCAGGACAATCAGGGTGGTG; reverse primer GGAGAAGTGCGGAGATTCAACA. Quantitative RT-PCR was performed in triplicate using 1 μl of cDNA template in a 50 μl reaction. The linearity and efficiency of PCR amplifications were assessed using standard curves generated by serial dilution of cDNA; in addition, melt curve analysis was used to confirm the specificity of amplification and absence of primer dimers. In all samples, the relative expression of each target gene respect to the control (reference sample) was evaluated by the comparative threshold cycle (ΔCt) method. All values were normalized to the 18S rRNA housekeeping gene.

2.6. Mn-SOD, GPx and CAT protein expression

The expression of the antioxidant enzymes was evaluated by Western blotting. Equal amounts (35 μg/sample) of tissue homogenates were separated on 12% SDS-PAGE, transferred to polyvinylidine difluoride (PVDF) membranes (Millipore, MA, USA) and immunoblotted with either polyclonal anti-SOD2 (1:1000, sc-30080), polyclonal anti-GPx (1:1000, sc-30147) or polyclonal anti-CAT (1:1000, sc-34282) (Santa Cruz Biotech, Santa Cruz, CA, USA) and subsequently with anti-rabbit (1:20,000 for SOD2 or 1:10000 for GPx, sc-2004) or -goat (1:3000 for CAT, sc-2033) horseradish peroxidase-conjugated antibodies (Santa Cruz Biotech, Santa Cruz, CA, USA). The immunoreactive bands were detected by chemiluminescence Immobilion Western ERP Substrate (Millipore, MA, USA) and quantified by densitometric analysis using a Gel Logic 2200 Imaging System and a Kodak Molecular Imaging Software (Kodak, CT, USA). GAPDH (1:5000, sc-25778, Santa Cruz Biotech, Santa Cruz, CA, USA) was used as a reference for equal protein loading.

2.7. Assessment of CAT and GPx phosphorylation

To assess CAT and GPx phosphorylation, the same membrane used for evaluating protein expression was stripped and reprobed with mouse monoclonal anti-phosphotyrosine (p-Tyr) antibody (1:1000, sc-7020, Santa Cruz Biotechnology, Santa Cruz, CA, USA) and anti-mouse (1:5000, sc-2005) horseradish peroxidase-conjugated secondary antibody (Santa Cruz Biotechnology, Santa Cruz, , CA, USA).

2.8. Antioxidant enzyme activities

2.8.1. CAT activity assay

Seventy micrograms of tissue homogenates was added to 100 mM phosphate buffer, pH 6.8, containing 10 mM H_2O_2. CAT activity was determined by the procedure of Aebi [24], following the decrease in absorbance at 240 nm of H_2O_2 for 30 s at 25 °C. The activity was calculated using a H_2O_2 extinction coefficient of 43.6×10^3 $M^{-1} \times cm^{-1}$.and was expressed as μmol/min/mg of protein.

2.8.2. GPx activity assay

Seventy micrograms of tissue homogenate was added to 100 mM phosphate buffer, pH 7.4, containing 0.5 mM EDTA, 1.0 mM NaN_3, 0.25 mM NADPH, 2.25 mM GSH, 1.0 U/ml glutathione reductase. After addition of 0.24 mM tert-butil hydroperoxide (Sigma, Italy), the change in optical density of NADPH was monitored spectrophotometrically at 340 nm for 2.0 min at 25 °C [23]. GPx activity was calculated using a molar extinction coefficient for NADPH of 6.22×10^3 $M^{-1} \times cm^{-1}$ and expressed as nmol/min/mg protein.

2.8.3. Mn-SOD activity assay

Mn-SOD activity was evaluated in 10 μg of tissue homogenate using a Chemical Superoxide Dismutase Assay kit (Cayman Chemical, Ann Arbor, MI, USA) as previously described [23] and expressed as U/mg protein.

2.9. Lipid peroxidation

Oxidative stress was detected by measuring malondialdehyde (MDA) concentration, as a marker of lipid peroxidation. A Bioxytech LPO-586 (Oxis International Inc, Prodotti Gianni, Italy) was used to this purpose.

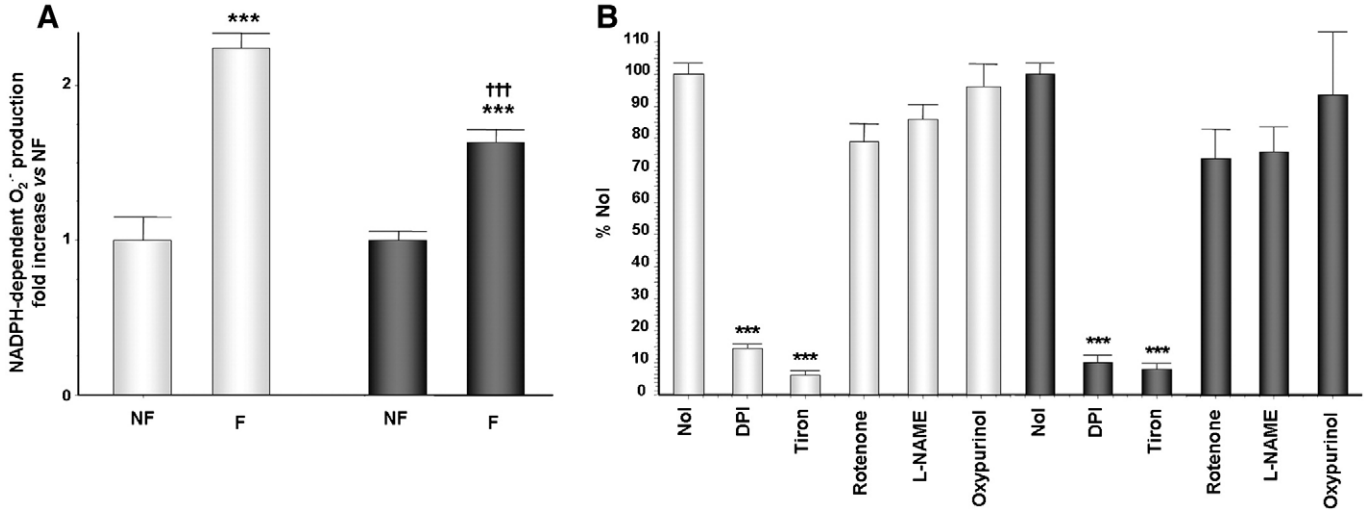

Fig. 1. NADPH-dependent superoxide production in human RV (open bars) and LV (solid bars) from non-failing (NF) and failing (F) hearts detected by lucigenin chemiluminescence. (A). Data are presented as mean ± SEM and expressed as fold increase calculated by normalizing values obtained in failing ventricles to average data from NF; $n = 7$ NF and $n = 12$ failing (F) ventricles from hearts with IHD or DCM; ***$p < 0.001$ vs. NF; †††$p < 0.001$ vs. failing RV. MLU, mean arbitrary light units. (B) Effect of specific oxidases inhibitors on NADPH-dependent superoxide production in RV and LV from human failing hearts. Data are presented as mean ± SEM and expressed as percentage of the value measured in the absence of inhibitors (NoI); ***$p < 0.001$ vs. NoI.

2.10. Statistical analysis

All values are expressed as mean ± SEM. Student's *t*-test was used for statistical analysis of the data. Correlation was obtained using a linear (Pearson) correlation test. Probabilities of $p<0.05$ were considered statistically significant.

3. Results

The results of all experiments did not differ according to the etiology of heart disease. Thus, in the following sections, the study population is grouped in failing and non-failing hearts.

3.1. Increased NADPH oxidase in failing right and left ventricles

In our previous work [10], we provide evidence that NADPH oxidase was the major source of ROS in human end-stage myocardium. In the present study, we confirmed a significant increase in NADPH-dependent superoxide production activity in both failing ventricles (RV: 291.7 ± 12.7 MLU/sec/mg; LV: 359.0 ± 18.0 MLU/sec/mg;) as compared with NF controls (RV: 132.8 ± 16.6 MLU/sec/mg; LV: 227.1 ± 10.1 MLU/sec/mg; $p<0.001$, F vs. NF). Notably, this increase was significantly higher in the failing RV (2.20-fold) than in the LV (1.58-fold) ($p<0.001$) (Fig. 1A). Moreover, NADPH-dependent superoxide production was greatly reduced in both failing ventricles only in the presence of the NADPH oxidase inhibitor diphenyleneiodonium (DPI) and of the O_2^- scavenger Tiron, whereas it was unaffected by the xanthine oxidase inhibitor oxypurinol, by a NOS inhibitor (L-NAME), or by the inhibitor of the mitochondrial electron transport chain, rotenone, supporting the main superoxide production attributable to NADPH oxidase activity (Fig. 1B).

3.2. Nox4 mRNA in failing right and left ventricles

To elucidate the mechanisms underlying the increased NADPH oxidase (Nox) activity in failing hearts, in a recent work we focused on Nox2, a catalytic subunit responsible for activity of the oxidase in cardiac cells, and its regulatory subunit $p47^{phox}$. To address the question whether different NADPH oxidase isoforms may account for regional (i.e., RV vs. LV) differences in ROS production, in this study we analyzed the expression of the other cardiac isoform of NADPH oxidase, Nox4. No significant differences emerged between RV and LV samples. In fact, Nox4 mRNA (Fig. 2) was unchanged in both failing ventricles as compared to NF. These results strengthen the findings previously reported [10] that increased oxidative stress due to NADPH oxidase is mainly attributable to post-transcriptional mechanisms.

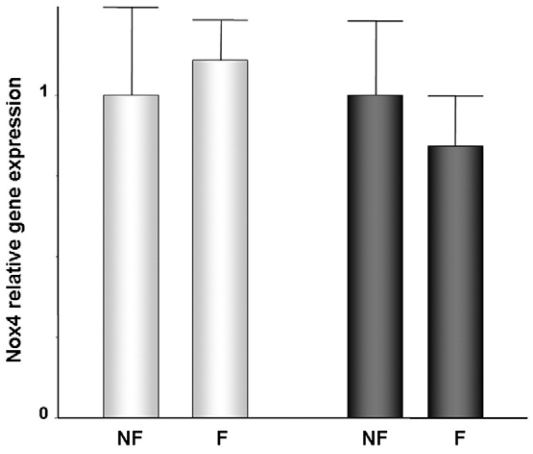

Fig. 2. Nox4 gene expression in human RV (open bars) and LV (solid bars) from non-failing (NF) and failing (F) hearts evaluated by real-time quantitative RT-PCR. Data are presented as mean ± SEM and expressed as fold increase relative to NF (NF = 1); $n=7$ NF and $n=12$ failing ventricles from hearts with IHD or DCM.

3.3. Antioxidant enzymatic defenses

We measured the mRNA and protein levels as well as the activities of H_2O_2 scavenging enzymes CAT, GPx and Mn-SOD. As shown in Fig. 3, CAT mRNA (Fig. 3A) and protein levels (Fig. 3B), assessed by

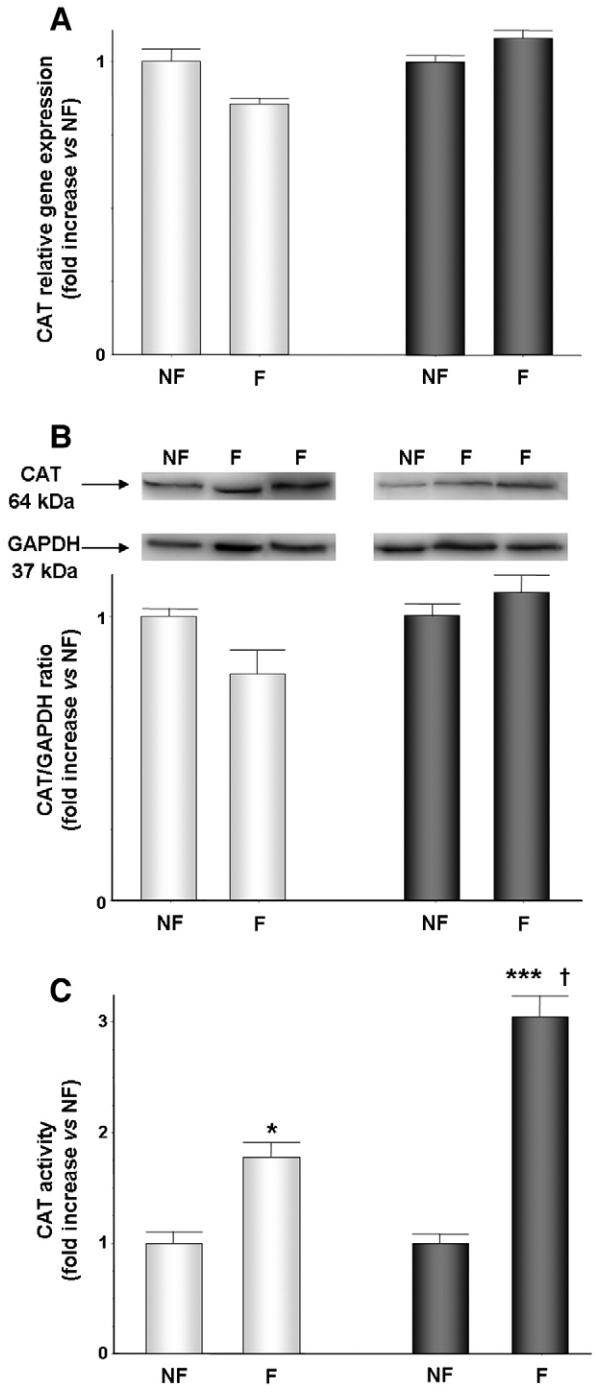

Fig. 3. Catalase (CAT) gene expression, protein expression and catalytic activity in human RV (open bars) and LV (solid bars) from non-failing (NF) and failing (F) hearts. CAT gene expression was evaluated by real-time quantitative RT-PCR (A). Representative immunoblot (upper) and densitometric quantification (lower) of ratio of CAT to GAPDH protein expression (B). CAT enzymatic activity (C). Data are presented as mean ± SEM and expressed as fold increase relative to NF (NF = 1). $n=7$ NF and $n=12$ failing heart ventricles from hearts with IHD or DCM. *$p<0.05$ vs. NF; ***$p<0.001$ vs. NF; †$p<0.05$ failing LV vs. failing RV.

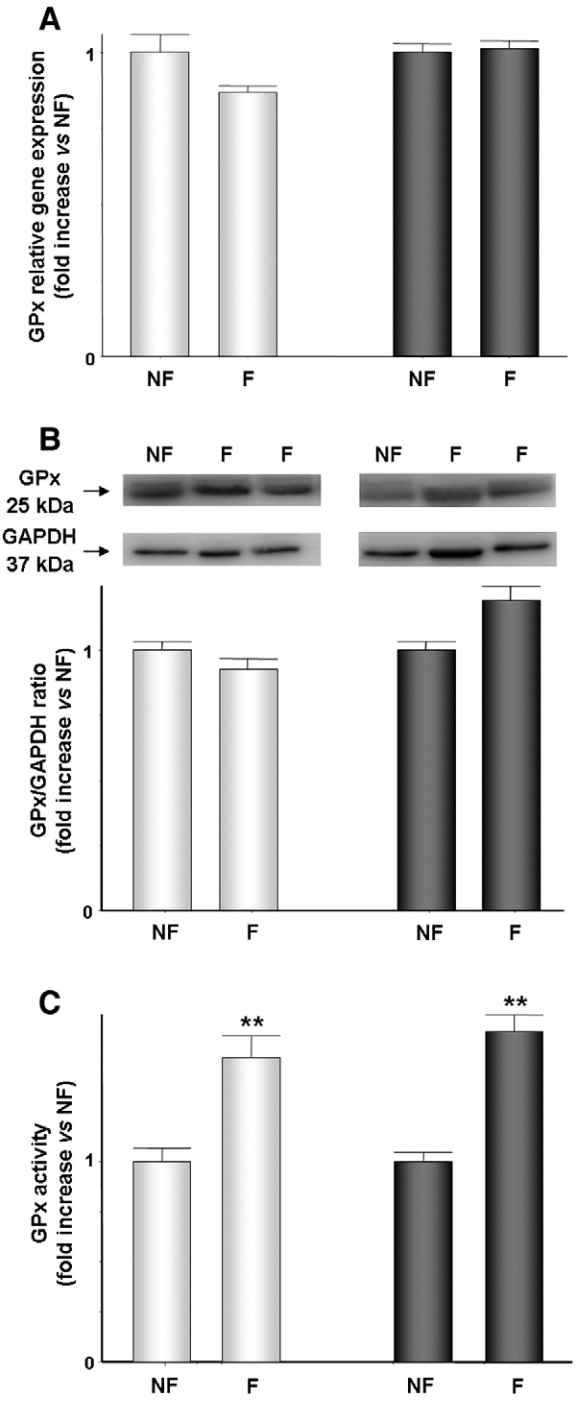

Fig. 4. Glutathione peroxidase (GPx) gene expression, protein expression and catalytic activity in human RV (open bars) and LV (solid bars) from non-failing (NF) and failing (F) hearts. GPx gene expression was evaluated by real time quantitative RT-PCR (A). Representative immunoblot (upper) and densitometric quantification (lower) of ratio of GPx to GAPDH protein expression (B). GPx enzymatic activity (C). Data are presented as mean ± SEM and expressed as fold increase relative to NF (NF = 1); $n = 7$ NF and $n = 12$ failing ventricles from hearts with IHD or DCM; $^{**}p < 0.01$ vs. NF.

densitometric analysis, were not significantly different in NF and failing RV and LV. In contrast, the enzymatic activity of CAT was significantly elevated in both ventricles from failing hearts. Such an increase was more evident in the LV (LV 3.04-fold $p < 0.001$; RV 1.76-fold, $p < 0.05$; F vs. NF) (Fig. 3C). In addition, in failing hearts the absolute levels of CAT activity in the LV (23.88 ± 1.50 μmol/min/mg protein) were significantly higher than in the RV (17.13 ± 1.29 μmol/min/mg protein) ($p < 0.05$; LV vs. RV).

Similar to CAT, GPx levels were stable in terms of mRNA levels (Fig. 4A) and protein content. The 23 kDa band from failing RV and LV samples, representing the GPx monomer [11], appeared unchanged with respect to NF, as confirmed by densitometric analysis (Fig. 4B). Instead, a significant and parallel increase of GPx activity was observed in failing RV and LV with respect to NF hearts (RV 1.52-fold, $p < 0.01$; LV 1.65-fold, $p < 0.01$; F vs. NF) (Fig. 4C).

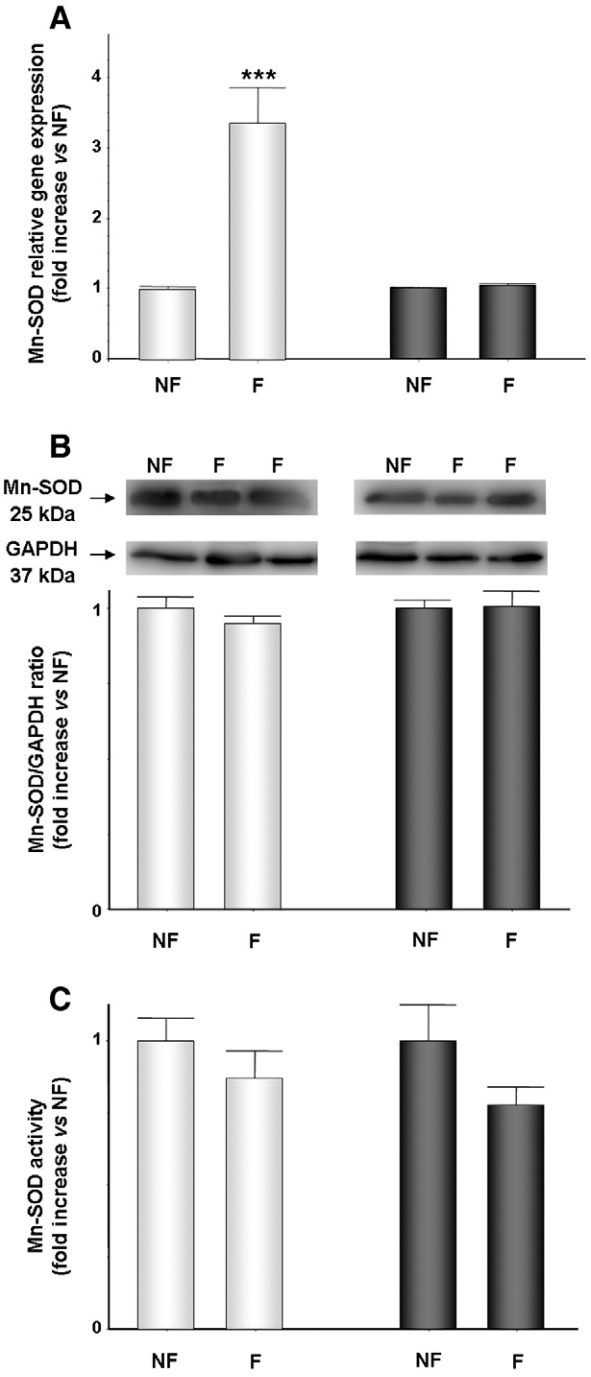

Fig. 5. Mn-Superoxide Dismutase (Mn-SOD) gene expression, protein expression and catalytic activity in human RV (open bars) and LV (solid bars) from non-failing (NF) and failing (F) hearts. Mn-SOD gene expression was evaluated by real-time quantitative RT-PCR (A). Representative immunoblot (upper) and densitometric quantification (lower) of ratio of Mn-SOD to GAPDH protein expression (B). Mn-SOD enzymatic activity (C). Data are presented as mean ± SEM and are expressed as fold increase relative to NF (NF = 1); $n = 7$ NF and $n = 12$ failing ventricles from hearts with IHD or DCM; $^{***}p < 0.001$ vs. NF.

Mn-SOD mRNA level was increased in the failing RV (5.87-fold *vs.* NF RV) but not in the failing LV (Fig. 5A), whereas Mn-SOD protein expression (Fig. 5B) and its enzymatic activity were unchanged in both failing ventricles (Fig. 5C).

Overall, these findings suggest that a consistent, similar adaptive response does occur in human failing LV and RV, as far as the enzymatic activity is concerned. This increase in antioxidant enzyme activities, more evident in failing LV (in particular for CAT), seems to be largely attributable to post-translational modifications likely induced by oxidative stress.

3.4. Tyrosine (Tyr) phosphorylation in failing RV and LV

Recently, oxidative stress has been shown to activate the Abl family of mammalian non-receptor tyrosine kinases resulting in increased CAT and GPx phosphorylation and activity [25]. To determine whether the observed increases in CAT and GPx activity in our failing samples could be attributed to Tyr phosphorylation, the same membrane used to analyze CAT and GPx protein expression was subsequently blotted with an anti-phospho-Tyr antibody. Interestingly, for both enzymes the bands corresponding to failing RV and LV showed a significant increases in Tyr phosphorylation with respect to NF ones. Moreover, the increase in CAT phosphorylation was significantly ($p<0.05$) higher in LV than RV, whereas no difference was observed between the two ventricles in GPx phosphorylation (Fig. 6), thus suggesting that changes in Tyr phosphorylation and enzyme activities go hand-in-hand.

3.5. Correlation between NADPH oxidase and antioxidant enzyme activities

In order to verify a possible link between oxidative stress and antioxidant enzyme activation, we correlated the activity of NADPH oxidase with that of GPx and CAT in the RV and LV. As shown in Fig. 6, a significantly positive correlation was found between the values of the GPx (RV: $r=0.6897$, $p=0.0091$; LV: $r=0.8744$, $p=0.0001$) (Fig. 7A) and CAT (RV: $r=0.8142$, $p<0.0007$; LV: $r=0.7784$, $p<0.0001$) (Fig. 7B) and that of NADPH oxidase in the LV and RV. Interestingly, the slope of the linear correlation (m) appeared to be steeper in the LV than in RV for both GPx (LV: $m=2.416$; RV: $m=1.485$) and CAT (LV: $m=1.007$; RV: $m=0.354$), suggesting that the oxidative stress promotes antioxidant adaptive responses more intensively in LV versus RV.

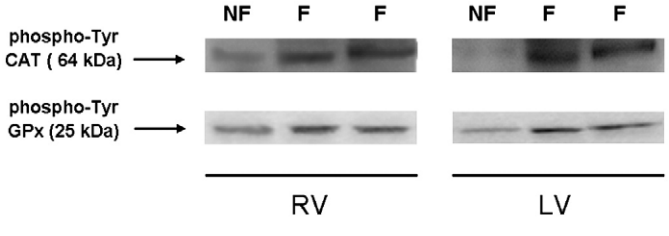

	RV	LV
CAT phospho-Tyr n-fold (F *vs* NF)	1.59 ± 0.05***	2.20 ± 0.21*†
GPx phospho-Tyr n-fold (F *vs* NF)	1.59 ± 0.16*	1.75 ± 0.15**

*p<0.05, **p<0.01, ***p<0.001 F *vs* NF. †p<0.05 failing LV *vs* failing RV

Fig. 6. CAT and GPx tyrosine (Tyr) phosphorylation in human RV and LV from non-failing (NF) and failing (F). Representative immunoblot (upper) and densitometric quantification related to GAPDH expression, shown, respectively, in Fig. 3 for CAT and in Fig. 4 for GPx, (lower) of phosphorylation expressed as fold increase of F relative to NF (NF = 1) ventricles. $n=5$ NF and $n=5$ failing ventricles from hearts with IHD or DCM.

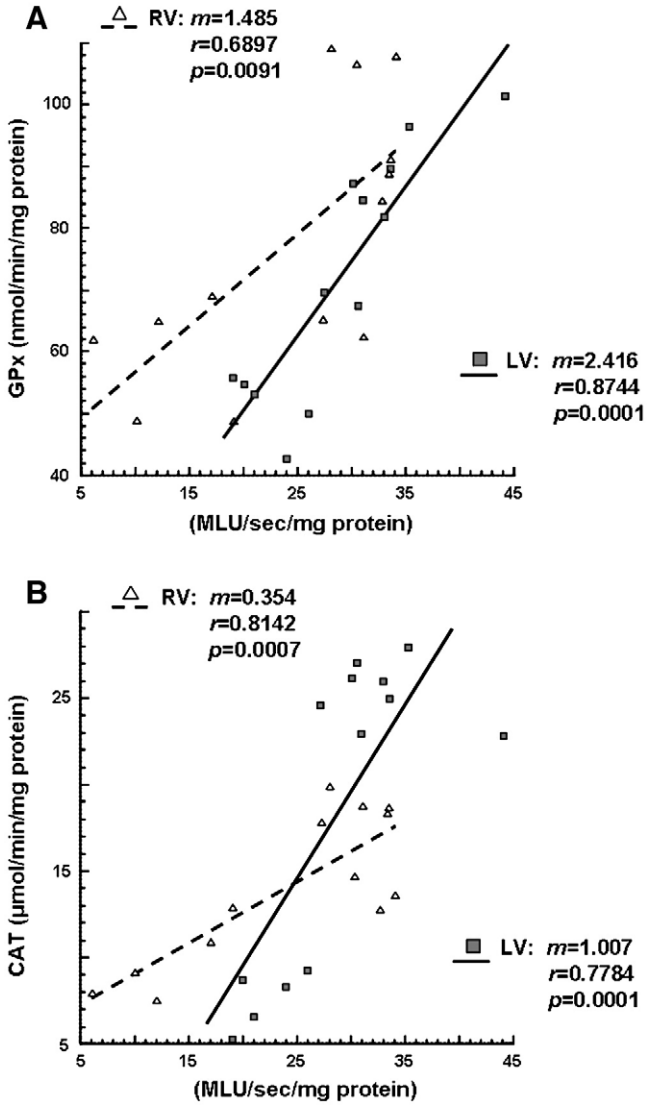

Fig. 7. Correlations between NADPH-dependent superoxide production (x axis) and GPx (A) or CAT (B) enzymatic activity (y axis) of NF and failing hearts; $n=5$ NF and $n=8$ failing ventricles from hearts with IHD and DCM. NADPH-dependent superoxide production is expressed as MLU/s/mg protein (MLU, Mean Light Unit). GPx activity is expressed as nmol/min/mg protein. CAT activity is expressed as µmol/min/mg protein.

3.6. Lipid peroxidation

Consistent with the differences observed in antioxidant enzymes activities, the MDA levels, measured as an indirect marker of oxidative stress, were significantly increased in both ventricles from failing hearts. However, diseased RV exhibited a marked rise in lipoperoxidative damage as compared to the NF control (RV: 1.95-fold; LV: 1.64-fold); in addition, the latter resulted significantly higher than that of diseased LV.

4. Discussion

In this study, we reported that, in human failing hearts, the increased ROS generation by NADPH oxidase is associated with enhanced activity of two antioxidant enzymes. This adaptive response mainly occurs through a post-translational modification and appears more marked in the LV. NADPH oxidase activity and lipid peroxidation are higher in RV than LV. Thus, RV might be less protected against oxidative stress damage.

4.1. NADPH oxidase activity and its regulation

The results showed in this study extend our previous observations on NADPH oxidase activation in human failing heart [10]. Although other contribution in ROS generation cannot be ruled out, we confirmed a NADPH-dependent oxidase system as a major source of O_2^- production in human failing hearts and shed light on the molecular mechanisms underlying its increased activation. NADPH oxidase is a multimeric enzyme that contains a core membrane-bound flavocytochrome comprising a catalytic Nox subunit and a lower molecular weight $p22^{phox}$ subunit. Five distinct Nox isoforms (Nox1–5) are expressed in a tissue-specific pattern, Nox2 and Nox4 being the main isoforms expressed in cardiac cells [26]. Nox2 oxidase activation requires the association of the cytosolic regulatory units ($p67^{phox}$, Rac, $p47^{phox}$ and $p40^{phox}$) with the flavocytochrome [3]. At variance with Nox2, Nox4 is constitutively active and has been suggested to be regulated mainly at the transcriptional level [27]. NADPH oxidase activation in response to hypertrophic stimuli (angiotensin II, epinephrine and mechanical overload) [28–31] occurs through either increased expression or post-translational modifications (by protein kinase c and/or Src kinase) and regulatory subunit translocation (notably $p47^{phox}$ and /or Rac) [4,10,32–35]. Our previous data showed that Nox2 protein expression did not differ between NF and failing hearts, whereas both $p47^{phox}$ overexpression and membrane translocation were increased with a higher $p47^{phox}$ membrane/cytosol ratio in failing RV than LV [27]. To get further insight into NADPH regulatory mechanisms, we analyzed the expression of Nox4 in both failing ventricles. We did not observe any increase in its expression, with Nox4 mRNA levels being unchanged in failing ventricles with respect to NF ones. Overall, these results suggest a prominent role of post-transcriptional mechanisms in NADPH oxidase activation, in agreement with our previous finding [10].

4.2. Antioxidant enzymes and their regulation

A major contribution of our results is the characterization of the mutual relationship between oxidant and antioxidant activity in the RV and LV from human failing hearts. Despite a marked increase of CAT and GPx activities, mRNA expression and protein levels were unchanged for both enzymes. These findings support the hypothesis that a dissociation might occur between mRNA/protein expression and activity, suggesting that the adaptive response to increased oxidative stress does not lead to increase transcription of these antioxidant enzymes but may reflect a post-translational modification. NADPH oxidase ROS generation may mediate its effects through different downstream signaling pathways including the activation of redox-sensitive kinases [7–10]. In our previous investigations, we demonstrated that in end-stage hearts and in cardiomyoblasts exposed to simulated I/R conditions an increased NADPH oxidase activity was significantly related with enhanced lipid peroxidation and activation of redox sensitive kinases [36].

In this study, we established a significant correlation between NADPH-dependent ROS production and antioxidant enzyme activity in failing RV and LV. Furthermore, for both CAT and GPx activities, the slope of the linear correlation appeared steeper in LV than in RV. On the other hand, MDA levels, that some other authors related to ventricular contractile dysfunction [37], were significantly higher in failing RV than LV. Taken together, these findings suggested that LV might be more protected against oxidative stress.

Although the molecular mechanism underlying CAT (or GPx) activation cannot be thoroughly investigated in this setting, recent evidence in literature and our present results allow to infer a role for protein Tyr-phosphorylation. In fact, Cao et al. [38,39] reported that in vitro exposure to hydrogen peroxide activates the Abl family of mammalian non-receptor tyrosine kinases, including c-Abl and Arg. Such activation was associated with CAT and GPx phosphorylation and their subsequent activity stimulation. In our samples, we found an increase in CAT and GPx Tyr-phosphorylation in both failing ventricles and, interestingly, the levels of these increases go hand-in-hand with those of respective enzyme activities. To our knowledge, this is the first evidence suggesting that such a mechanism may work in human heart disease. So, although speculative, for the limitation on finding a clear evidence for a cause–effect relationship in end-stage hearts, it is reasonable to hypothesize that increased NADPH oxidase ROS production, as it activated redox sensitive kinases may activate c-Abl and Arg kinases with the subsequent stimulation of the CAT and GPx catalytic activities, a mechanism that may contribute to normalize the level of oxidative stress.

At variance with CAT and GPx, and in line with previous study [23], protein expression and enzymatic activity for Mn-SOD were unchanged in failing ventricles, suggesting that this mitochondrial enzyme may be not involved in the adaptive response to NADPH-dependent oxidative stress in human heart failure. The observation of an upregulation of Mn-SOD gene only in the right ventricle is intriguing, and may reflect “site-related” mitochondrial differences, that deserve additional investigation.

4.3. Conclusions and limitations

A mechanicistic interpretation of our results is prevented by the usage of human samples from end-stage failing hearts; thus, the contribution of post-translational modifications, in particular Tyr phosphorylation, to the adaptive antioxidant response in human heart disease remains to be established.

Overall, our findings show that the molecular and biochemical mechanisms for cardiac failure although qualitatively similar, may be quantitatively different in the right and left ventricle and suggest that RV might be more vulnerable than LV against oxidative stress. In this perspective, as recently pointed out [15], our study is in keeping with a potential contribution of RV alterations to the progression toward overt heart failure, and the expectation that gathering information on RV maladaptation may translate into better treatment and prevention.

Acknowledgments

The financial support of Ministero dell'Istruzione, dell'Università e della Ricerca (M.I.U.R) and of Ente Cassa di Risparmio di Firenze is gratefully acknowledged.

References

[1] J.A. Byrne, D.J. Grieve, A.C. Cave, A.M. Shah, Oxidative stress and heart failure, Arch. Mal. Coeur Vaiss. 96 (2003) 214–221.
[2] F.J. Giordano, Oxygen, oxidative stress, hypoxia, and heart failure, J. Clin. Invest. 115 (2005) 500–508.
[3] C. Heymes, J.K. Bendall, P. Ratajczak, A.C. Cave, J.L. Samuel, G. Hasenfuss, A.M. Shah, Increased myocardial NADPH oxidase activity in human heart failure, J. Am. Coll. Cardiol. 41 (2003) 2164–2171.
[4] J.M. Li, N.P. Gall, D.J. Grieve, M. Chen, A.M. Shah, Activation of NADPH oxidase during progression of cardiac hypertrophy to failure, Hypertension 40 (2002) 477–484.
[5] S. Dieterich, U. Bieligk, K. Beulich, G. Hasenfuss, J. Prestle, Gene expression of antioxidative enzymes in the human heart, Circulation 101 (2000) 33–39.
[6] F.M. Hill, P.K. Singal, Antioxidant and oxidative stress changes during heart failure subsequent to myocardial infarction in rats, Am. J. Pathol. 148 (1996) 291–300.
[7] A. Akki, M. Zhang, C. Murdoch, A. Brewer, A.M. Shah, NADPH oxidase signaling and cardiac myocyte function, J. Mol. Cell. Cardiol. 47 (2009) 15–22.
[8] R. Dworakowski, N. Anilkumar, M. Zhang, A.M. Shah, Redox signalling involving NADPH oxidase-derived reactive oxygen species, Biochem. Soc. Trans. (2006) 34.
[9] C. Murdoch, M. Zhang, A. Cave, A. Shah, NADPH oxidase-dependent redox signalling in cardiac hypertrophy, remodelling and failure, Cardiovasc. Res. 71 (2006) 208–215.
[10] C. Nediani, E. Borchi, C. Giordano, S. Baruzzo, V. Ponziani, M. Sebastiani, P. Nassi, A. Mugelli, G. d'Amati, E. Cerbai, NADPH Oxidase-dependent redox signaling in human heart failure: relationship between the left and right ventricle, J. Mol. Cell. Cardiol. 42 (2007) 826–834.

[11] A.T. Baumer, M. Flesch, X. Wang, Q. Shen, Z.G. Feuerstein, M. Bohm, Antioxidative enzymes in human hearts with idiopatic dilated cardiomyopathy, J. Mol. Cell. Cardiol. 32 (2000) 121–133.
[12] F. Sam, D. Kerstetter, D. Pimental, S. Mulukutla, A. Tabaee, M. Bristow, W. Colucci, D. Sawyer, Increased reactive oxygen species production and functional alterations in antioxidant enzymes in human failing myocardium, J. Card. Fail. 11 (2005) 473–480.
[13] A. Brieke, D. DeNofrio, Right ventricular dysfunction in chronic dilated cardiomyopathy and heart failure, Coron. Artery Dis. 16 (2005) 5–11.
[14] F. Haddad, S.A. Hunt, D.N. Rosenthal, D.J. Murphy, Right ventricular function in cardiovascular disease: Part I. anatomy, physiology, aging, and functional assessment of the right ventricle, Circulation 117 (2008) 1436–1448.
[15] N. Voelkel, R. Quaife, L. Leinwand, R. Barst, M. McGoon, D. Meldrum, J. Dupuis, C. Long, L. Rubin, F. Smart, Y. Suzuki, M. Gladwin, E. Denholm, D. Gail, National Heart, Lung and Blood Institute Working Group on cellular and molecular mechanisms of right heart failure, right ventricular function and failure. Report of a National Heart, Lung and Blood Institute Working Group on cellular and molecular mechanisms of right heart failure, Circulation 114 (2006) 1883–1891.
[16] F.M. Hill, P.K. Singal, Right and left myocardial antioxidant responses during heart failure subsequent to myocardial infarction, Circulation 96 (1997) 2414–2420.
[17] L. Liu, L. Marcocci, C. Wong, A. Park, Y. Suzuki, Serotonin-mediated protein carbonylation in the right heart, Free Rad. Biol. Med. 45 (2008) 847–854.
[18] P. Modesti, S. Vanni, I. Bertolozzi, I. Cecioni, C. Lumachi, A. Perna, M. Boddi, G. Gensini, Different growth factor activation in the right and left ventricles in experimental volume overload, Hypertension 43 (2004) 101–108.
[19] N. Dang, V. Topkara, M. Mercando, J. Kay, K.H. Kruger, M.S. Aboodi, M.C. Oz, Y. Naka, Right heart failure after left ventricular assist device implantation in patients with chronic congestive heart failure, J. Heart Lung Transplant. 25 (2006) 1–6.
[20] A. Barbone, J. Holmes, P. Heerdt, A. The', Y. Naka, N. Joshi, M. Daines, A.R. Marks, M.C. Oz, D. Burkhoff, Comparison of right and left ventricular responses to left ventricular assist device support in patients with severe heart failure: a primary role of mechanical unloading underlying reverse remodeling, Circulation 104 (2001) 670–675.
[21] S. Klotz, A. Barbone, S. Reiken, J. Holmes, Y. Naka, M.C. Oz, A.R. Marks, D. Burkhoff, Left ventricular assist device support normalizes left and right ventricular beta-adrenergic pathway properties, J. Am. Coll. Cardiol. 45 (2005) 668–676.
[22] S. Puwanant, K. Hamilton, C. Klodell, J. Hill, R. Schofield, T. Cleeton, D. Pauly, J. Aranda, Tricuspid annular motion as a predictor of severe right ventricular failure after left ventricular assist device implantation, J. Heart Lung Transplant. 27 (2008) 1102–1107.
[23] M. Sebastiani, C. Giordano, C. Nediani, C. Travaglini, E. Borchi, M. Zani, M. Feccia, M. Mancini, V. Petrozza, A. Cossarizza, P. Gallo, R. Taylor, G. d'Amati, Induction of mitochondrial biogenesis is a maladaptive mechanism in mitochondrial cardiomyopathies, J. Am. Coll. Cardiol. 50 (2007) 1362–1369.
[24] H. Aebi, Catalase in vitro, Methods Enzymol. 105 (1984) 121–126.
[25] S. Rhee, K. Yang, H. Woo, T. Chang, Controlled elimination of intracellular H_2O_2: regulation of peroxiredoxin, catalase, and glutathione peroxidase via post-traslational modification, Antioxid. Redox Signal. 7 (2005) 619–626.
[26] K. Bedard, K.H. Krause, The NOX family of ROS-generating NADPH oxidases: physiology and pathophysiology, Physiol. Rev. 87 (2007) 245–313.
[27] J.D. Lambeth, NOX enzymes and the biology of reactive oxygen, Nat. Rev. Immunol 4 (2004) 181–189.
[28] C. Fiorillo, C. Nediani, V. Ponziani, L. Giannini, A. Celli, N. Nassi, L. Formigli, A.M. Perna, P.A. Nassi, Cardiac volume overload rapidly induces oxidative stress-mediated myocyte apoptosis and hypertrophy, Biochim. Biophys, Acta 1741 (2005) 173–182.
[29] J.M. Li, L.M. Fan, M.R. Christie, A.M. Shah, Acute tumor necrosis factor alpha signaling via NADPH oxidase in microvascular endothelial cells: role of p47phox phosphorylation and binding to TRAF4, Mol. Cell. Biol. 25 (2005) 2320–2330.
[30] J.M. Li, A.M. Shah, Mechanism of endothelial cell NADPH oxidase activation by angiotensin II. Role of the p47 phox subunit, J. Biol. Chem. 278 (2003) 12094–12100.
[31] L. Xiao, D. Pimentel, J. Wang, K. Singh, W. Colucci, D. Sawyer, Role of reactive oxygen species and NAD(P)H oxidase in alpha 1-adrenoceptor signaling in adult rat cardiac myocytes, Am. J. Physiol. Cell. Physiol. 282 (2002) C926–C934.
[32] R. Gupte, V. Vijay, B. Marks, R. Levine, H. Sabbah, M. Wolin, F. Recchia, S. Gupte, Upregulation of glucose-6-phosphate dehydrogenase and NAD(P)H oxidase activity increases oxidative stress in failing human heart, J. Card. Fail. 13 (2007) 497–506.
[33] C. Maack, T. Kartes, H. Kilter, H. Schafers, G. Nickenig, M. Bohm, U. Laufs, Oxygen free radical release in human failing myocardium is associated with increased activity of Rac1-GTPase and represents a target for statin treatment, Circulation 108 (2003) 1567–1574.
[34] F. Qin, R. Patel, C. Yan, W. Liu, NADPH oxidase is involved in angiotensin II-induced apoptosis in H9c2 cardiac muscle cells: effect of apocynin, Free Rad. Biol. Med. 40 (2006) 236–246.
[35] P. Seshiah, D. Weber, P. Rocic, L. Valppu, Y. Taniyama, K. Griendling, AngiotensinII , stimulation of NAD(P)H oxidase activity upstream mediators, Circ. Res. 91 (2002) 406–413.
[36] E. Borchi, M. Parri, L. Papucci, M. Becatti, N. Nassi, P. Nassi, C. Nediani, Role of NADPH oxidase in H9c2 cardiac muscle cells exposed to simulated ischemia-reperfusion, J. Cell. Mol. Med. (2008) Electronic publication ahead of print.
[37] D. Folden, A. Gupta, A. Sharma, S. Li, J. Saari, J. Ren, Malondialdehyde inhibits cardiac contractile function in ventricular myocytes via a p38 mitogen-activated protein kinase-dependent mechanism, Br. J. Pharmacol. 139 (2003) 1310–1316.
[38] C. Cao, Y. Leng, W. Huang, X. Liu, D. Kufe, Glutathione peroxidase 1 is regulated by the c-Abl and Arg tyrosine kinases, J. Biol. Chem. 278 (2003) 39609–39614.
[39] C. Cao, Y. Leng, D. Kufe, Catalase activity is regulated by c-Abl and Arg in the oxidative stress response, J. Biol. Chem. 278 (2003) 29667–29675.